The Astrophysical Journal, 651:676–687, 2006 November 10

RINGS AND BENT CHAIN GALAXIES IN THE GEMS AND GOODS FIELDS

Debra Meloy Elmegreen
Department of Physics and Astronomy, Vassar College, Box 745, Poughkeepsie, NY 12604; elmegreen@vassar.edu

and

Bruce G. Elmegreen
IBM Research Division, T. J. Watson Research Center, P.O. Box 218, Yorktown Heights, NY 10598; bge@watson.ibm.com
Received 2006 June 25; accepted 2006 July 21

ABSTRACT

Twenty-four galaxies with rings or partial rings were studied in the GEMS and GOODS fields out to $z \sim 1.4$. Most resemble local collisional ring galaxies in morphology, size, and clumpy star formation. Clump ages range from 10^8 to 10^9 yr, and clump masses go up to several $\times 10^8\,M_\odot$, based on color evolution models. The clump ages are consistent with the expected lifetimes of ring structures if they are formed by collisions. Fifteen other galaxies that resemble the arcs in partial ring galaxies but have no evident disk emission were also studied. Their clumps have bluer colors at all redshifts compared to the clumps in the ring and partial ring sample, and their clump ages are younger than in rings and partial rings by a factor of $\sim$10. In most respects, they resemble chain galaxies except for their curvature; we refer to them as "bent chains." Several rings are symmetric with centered nuclei and no obvious companions. They could be outer Lindblad resonance rings, although some have no obvious bars or spirals to drive them. If these symmetric cases are resonance rings, then they could be the precursors of modern resonance rings, which are only $\sim$30% larger on average. This similarity in radius suggests that the driving pattern speed has not slowed by more by $\sim$30% during the last $\sim$7 Gyr. Those without bars could be examples of dissolved bars.

Subject headings: galaxies: formation — galaxies: high-redshift — galaxies: interactions — galaxies: structure

1. INTRODUCTION

Outer rings in galaxies can be the result of plunging impacts, spiral and bar resonances, or satellite accretion onto a stable polar orbit. All types combined comprise less than 0.2% of local spiral galaxies (Athanassoula & Bosma 1985), although 4% of early-type galaxies in de Vaucouleurs & Buta (1980) have outer resonance rings. Galaxies with centrally located nuclei and smooth outer rings are sometimes referred to as "O-type," while those with knotty structure and occasionally offset nuclei are called "P-type" (Few & Madore 1986).

Collisional ring galaxies usually have a clumpy ring of star formation that is disk material compressed by a wave driven outward in response to the impacting galaxy's gravitational force (Lynds & Toomre 1976; Theys & Spiegel 1976, 1977; Appleton & Struck-Marcell 1987; Struck 1997). Generally the intruder is visible nearby and has a mass of at least $\sim$10% of the main galaxy mass (Lavery et al. 2004). Collisional ring galaxies may have nuclei or offset nuclei, or they could be empty inside with one prominent clump on the ring. All of these structures are expected to last for only a brief time, $\sim 10^8$ yr (Theys & Spiegel 1976, 1977).

The most famous example of a collisional ring galaxy is the Cartwheel (Fosbury & Hawarden 1977; Struck et al. 1996), which has an offset nucleus and a ring of recent star formation. A catalog of southern galaxies by Arp & Madore (1987) includes many examples of collisional ring galaxies. Individual collisional ring galaxies studied recently include Arp 107 (Smith et al. 2005), VII Zw 466 (Appleton et al. 1996), AM 0644−741 (Higdon & Wallin 1997), NGC 922 (Wong et al. 2006), and a sample of 11 galaxies including the Cartwheel (Appleton & Marston 1997). Numerical simulations of mergers have been used to reproduce many features of these nearby systems (e.g., review by Barnes & Hernquist 1992; Hernquist & Weil 1993; Mihos & Hernquist 1994; review by Struck 1999).

Resonance rings can be located near the nucleus, mid-disk, or outer disk, depending on the resonance (see reviews by Athanassoula & Bosma 1985; Buta & Combes 1996). Among local galaxies, the outer resonance rings prefer early-type spirals (de Vaucouleurs & Buta 1980). Polar rings are perpendicular to the central galaxy's plane and usually associated with S0 types.

Collisional ring galaxies should be relatively more common in the high-redshift universe, because interactions were more frequent in the past (e.g., Abraham et al. 1996b). The merger rate as a function of redshift has been studied from visible morphologies (Straughn et al. 2006), comoving densities of collisional ring galaxies (Lavery et al. 2004), Gini coefficients (Lotz et al. 2006), angular correlation functions (Neuschaefer et al. 1997), and asymmetry indices (Abraham et al. 1996a; Conselice et al. 2003). These studies find that the merger rate increases with redshift as $(1 + z)^n$ for n between 2 and 7.

The GEMS (Galaxy Evolution from Morphology and SEDs; Rix et al. 2004), GOODS (Great Observatories Origins Deep Survey; Giavalisco et al. 2004), and UDF (Ultra Deep Field; Beckwith et al. 2006) surveys done with the *Hubble Space Telescope* Advanced Camera for Surveys (*HST* ACS) have enabled unprecedented high-resolution studies of the morphology of intermediate and high-redshift galaxies. Here we examine the GEMS and GOODS fields for ring and partial ring galaxies, and we compare the properties of these galaxies to their local counterparts and to similar objects in the UDF.

2. DATA AND ANALYSIS

The UDF, GOODS, and GEMS images from the public archive were used for this study. They include exposures in four filters for UDF and GOODS: F435W (B_{435}), F606W (V_{606}), F775W (i_{775}), and F850LP (z_{850}); and two filters for GEMS (V and z). The images were drizzled to produce final archival images with a scale of

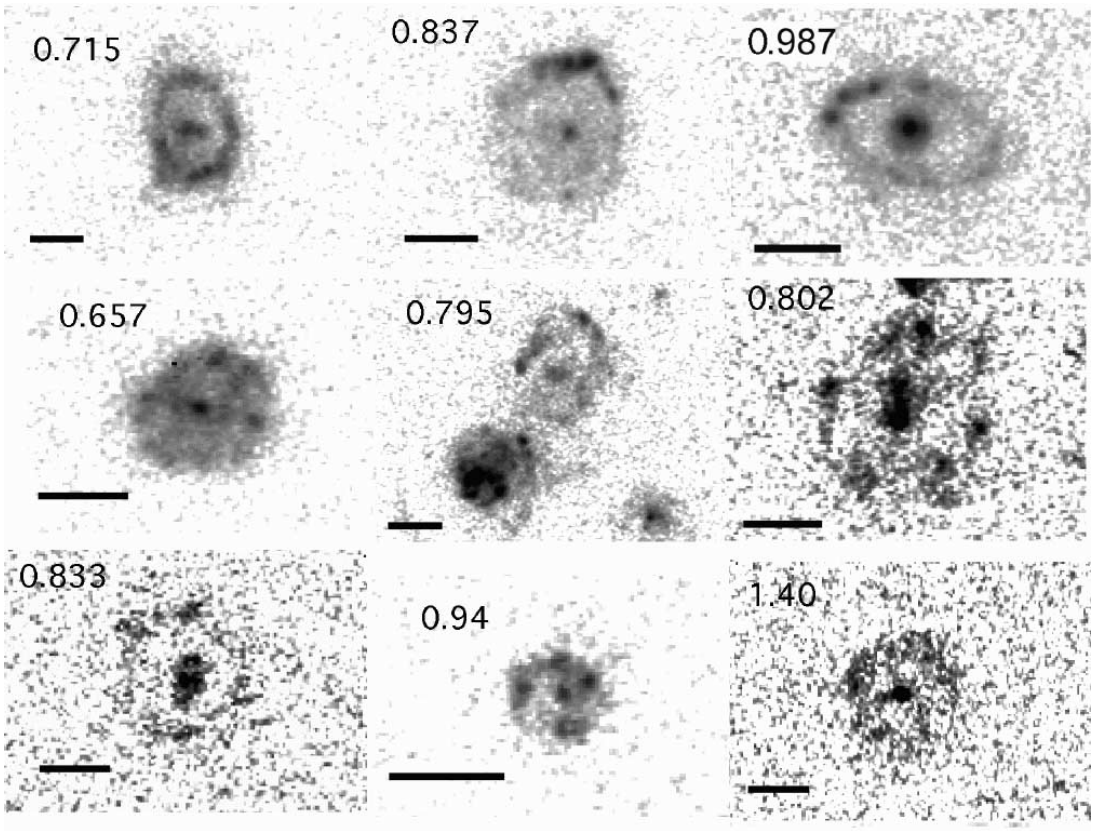

FIG. 1.—V_{606}-band images of ring galaxies in the GEMS and GOODS fields. Redshifts are in the upper left corner; horizontal lines represent 1″.

0.″03 pixel^{-1}. GEMS, which incorporates the southern GOODS survey (Chandra Deep Field South [CDF-S]) in the central quarter of its field, covers $28' \times 28'$; there are 63 GEMS and 18 GOODS images that make up the whole field. The GOODS images have a limiting AB magnitude of $V_{606} = 27.5$ for an extended object, or about 2 mag fainter than the GEMS images. The UDF is equivalent to one of these subfields, but probes to a depth of about 1.5 mag fainter than GOODS, or about 29 AB mag. There are over 25,000 galaxies catalogued for GEMS in the COMBO-17 survey (Classifying Objects by Medium-Band Observations, a spectrophotometric 17 filter survey; Wolf et al. 2003), as well as over 10,000 galaxies in the UDF (Beckwith et al. 2006).

We examined the GEMS and GOODS fields for ring galaxies, first using the online Skywalker images, and then using the 81 high-resolution V_{606} fits images. We chose a limiting diameter of $\sim$20 pixels because it is difficult to discern a ring structure in smaller galaxies; in fact, all of our rings are larger than 30 pixels. Snapshots of the ring galaxies in the V_{606} images are shown in Figure 1, and partial rings are in Figure 2. Redshifts and 1″ lengths are indicated.

The average redshift of our sample is 0.8 ± 0.3, where a V_{606} image corresponds to the rest-frame U band. We examined all the available passbands for comparison and found little difference in structure from band to band. The V_{606} images in the figures have the same rings, clumps, and nuclear structures as the z_{850} images, which correspond to the rest-frame B band on average. We show only the V_{850} images because they have higher signal-to-noise ratios. The bottom three galaxies in Figure 2 have slightly different morphologies, called RK (ring-knot) by Theys & Spiegel (1976); they have a very large clump on the ring (which may be the impacting galaxy) and no large clump inside the ring. In all, we selected 9 ring galaxies and 15 partial ring galaxies.

GEMS and GOODS redshifts were obtained from the COMBO-17 list (Wolf et al. 2003). The data are in Table 1, which gives the COMBO-17 catalog number and redshift for the galaxies in order of presentation in the figures. The redshift ranges from $z = 0.1$ to 1.4 in the surveyed area of 2.8×10^6 arcsec^2. For comparison, 25 collisional ring galaxies were identified by Lavery et al. (2004) in 162 WFPC2 (Wide Field and Planetary Camera) fields from $z = 0.1$ to 1, covering a comparable area of 4.2×10^6 arcsec^2. Our number per unit redshift and per unit solid angle is similar to theirs.

In the GEMS and GOODS fields, 15 other galaxies were found to resemble the clumpy arcs of partial ring galaxies, but they did not have nuclei or inner disks suggestive of a ring galaxy. They looked more like chain galaxies, which are common at intermediate to high redshift (Cowie et al. 1995). We refer to these 15 as "bent chain" galaxies. Their properties are listed in Table 1, and they are shown in Figure 3, with 2 σ contour images in Figure 4 that highlight the faintest structures. Some bent chain galaxies could have suffered collisions like those in collisional ring galaxies, as indicated by the wide variety of shapes for direct hits shown by Struck (1999). In particular, Struck simulates "banana" shapes reminiscent of bent chains, in addition to partial rings reminiscent of the galaxies in Figure 2. It is not clear from the morphology alone whether bent chains are the same as partial rings (we consider this difference in more detail below).

To help understand these bent chains, we compared them to straight chain galaxies and clump cluster galaxies, which are presumably face-on versions of chain galaxies. We identified 19 chain galaxies in the GEMS and GOODS fields and added 29 chain and 44 clump cluster galaxies in the UDF. The UDF galaxies came from our morphology catalog of the UDF, where we classified 884 galaxies larger than 10 pixels in diameter into one of six main morphological types: chain, double, tadpole, clump

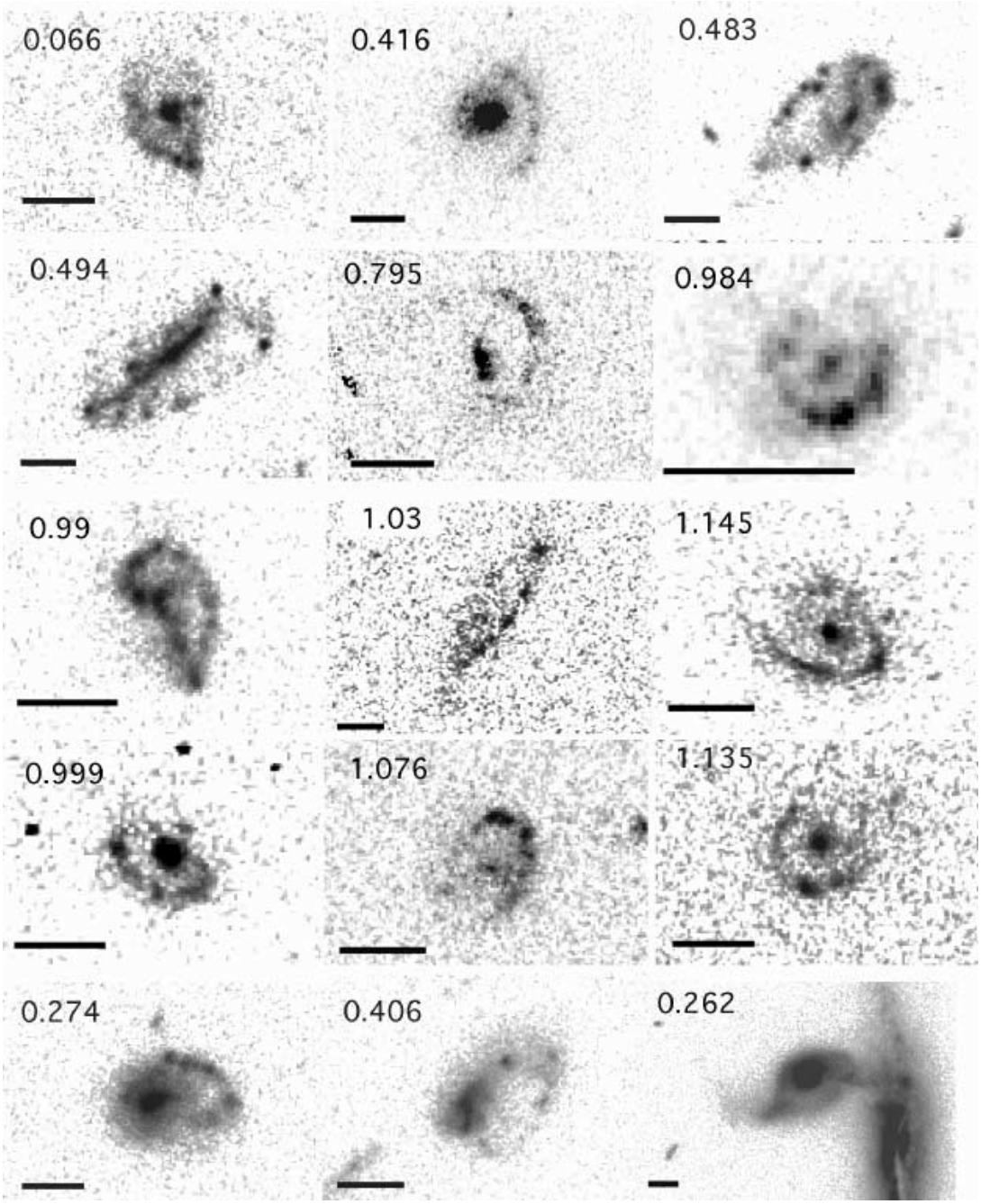

FIG. 2.—V_{606}-band images of partial ring galaxies in the GEMS and GOODS fields. Redshifts are in the upper left corner; horizontal lines represent 1″.

cluster, spiral, or elliptical (Elmegreen et al. 2005b). The photometric redshifts of the UDF galaxies were determined using the Bayesian photometric redshift (BPZ) method (Benitez 2000; Coe et al. 2006; Elmegreen et al. 2006). For the present study, we used only the UDF chains and clump clusters with $z < 1$, because the galaxies in our GEMS and GOODS surveys are primarily restricted to this regime.

Ellipse fits were done on the ring galaxies using the IRAF task `ellipse`. From these, average radial profiles were made to assess the light and color distributions. The IRAF task `pvector` was used to make intensity scans along the bent chain and chain galaxies.

Photometry was done on each prominent clump or nucleus in the GEMS and GOODS galaxies using the IRAF task `imstat`, in which a box was defined around each clump to measure the number of pixels and mean pixel count. Conversions to magnitudes were done using the zero points tabulated in the ACS data handbook.[1] Sky subtraction was not done because the background was negligible. The photometric errors are ~0.1–0.2 mag for individual clumps.

3. RESULTS

3.1. *Galaxy Properties*

The COMBO-17 table included rest-frame U, B, and V magnitudes for galaxies whose redshifts could be determined. Figure 5 shows the absolute rest-frame V magnitude as a function of redshift for the integrated galaxy light from rings and partial

[1] Available at http://www.stsci.edu/hst/acs/analysis/zeropoints.

TABLE 1
Ring and Bent Chain Galaxies

Catalog No.	Redshift z	Diameter (kpc)
Rings		
53346	0.715	11.5
47074[a]	0.837	17.9
44999[a]	0.987	20.9
58535[a]	0.657	12.3
50905	0.795	16.6
49092[a]	0.802	17.1
43780	0.833	14.9
25076[a]	0.94	7.6
62696	1.40	15.8
Partial Rings		
25065	0.066	2.0
36857	0.416	11.8
34409	0.483	16.0
48709	0.494	20.0
14373	0.795	13.1
21605	0.984	7.5
38657	0.99	13.0
34474	1.03	23.1
41925	1.145	13.4
34244	0.999	9.4
23459	1.076	11.3
36947	1.135	9.7
21635	0.274	9.5
29474	0.406	12.8
25874	0.262	19.4
Bent Chains[b]		
26239	0.048	1.4
27211	0.099	2.1
41096	0.113	2.9
11357	0.136	4.9
37539	0.296	14.9
30656	0.467	10.9
12329	0.703	8.8
48146	0.743	18.2
3618	0.764	26.6
23308	0.862	21.3
34857	1.007	36.5
54277	1.014	24.0
28154	1.153	10.9

[a] These galaxies have no companions 10 pixels or smaller in diameter that are within 3 galaxy diameters projected distance and within a redshift of 0.1. They are symmetric with centralized nuclei, so they are candidates for resonance ring galaxies. One of these, 49092, has a nucleus that appears slightly elongated and could be a bar.

[b] The last two galaxies in Fig. 3 are not listed in the COMBO-17 catalog.

rings (*filled circles*), bent chains (*triangles*), and chains (*open circles*) in the GEMS and GOODS fields (similar information has not been tabulated for the UDF galaxies). The galaxies range from absolute rest $V \sim -17$ to -22 mag. Three bent chains and one partial ring galaxy were eliminated from this figure because their small tabulated redshifts ($z < 0.1$) gave them absolute magnitudes of -12 to -14, which is not sensible considering their similarity in appearance and angular size to the other galaxies in our sample. The figure indicates that the ring and partial ring galaxies are $\sim$1.5 mag brighter at each redshift than the bent chain and chain galaxies.

The linear diameters of the galaxies (Table 1) were determined from their redshifts and observed angular diameters using the conversion for a ΛCDM cosmology (Carroll et al. 1992; Spergel et al. 2003). They are shown on the left in Figure 6 for the GEMS and GOODS galaxies (the right panel of the figure will be discussed in the next section). There is no correlation between minimum diameter and redshift, because the chosen galaxies were generally much larger than our size cutoff. The drop in size for very small redshifts could be the result of redshift errors, as discussed above, or it could be the result of a selection of GOODS and GEMS fields that avoid galaxies that are large in angular size. The range in size for the sample is comparable to the range for local galaxies. This rules out the possibility that the GEMS and GOODS rings studied here are circumnuclear, with the surrounding disks below the detection threshold.

Integrated rest-frame ($U-B$) and ($B-V$) colors are shown in Figure 7. The chain and bentchain galaxies in the GEMS field have colors similar to each other, and these are $\sim$0.5 mag bluer than the ring and partial ring galaxies, suggesting more recent star formation in the chains and bent chains. The colors of the ring and partial ring galaxies are typical for local galaxies with intermediate to late types (e.g., Fukugita et al. 1995), but the chain and bent chain galaxies are bluer than local late-type galaxies. These blue colors are consistent with the common observation that high-redshift galaxies of all types tend to be starbursting (Coe et al. 2006; Elmegreen et al. 2006; de Mello et al. 2006).

The radial profiles in V_{606} of the ring and partial ring galaxies were found to be approximately exponential in the inner regions out to the ring, suggesting that the underlying disks are the same as in local spirals. Inner exponentials also occur in local collisional ring galaxies. The ($V_{606}-z_{850}$) colors of our rings are 0.3 mag bluer than their average inner disks, suggesting enhanced ring star formation. Such blue colors are consistent with observations and models of the Cartwheel galaxy (Korchagin et al. 2001), VII Zw 466 (Thompson & Theys 1978), and other collisional ring galaxies (Appleton & Marston 1997). These local galaxies were observed in rest-frame $B-V$ and $V-K$, and not $U-B$ as in the present sample, but the relative blueness of the rings is the same for each.

In contrast, the bent chains generally have little emission inside their arcs, as is evident in Figure 4. Some bent chains have stray clumps nearby with approximately the same colors as the galaxies (e.g., galaxy No. 11357 in COMBO-17, which is the bent chain in Fig. 3 with redshift 0.136, and No. 3618 [$z = 0.764$]). A stray clump with the same redshift could be a collision partner, or it could be a remote part of the same disk that contains the bent chain. Some chains also have an asymmetry in the sharpness of their edges on the inner and outer arcs (e.g., COMBO-17 No. 3618 [$z = 0.764$] and No. 41096 [$z = 0.113$]), suggesting a disk or partial disk with the bent chain on the rim. Thus, the bent chains could be partial ring galaxies, but the galaxy disks around the bent chains would have to be unusually faint. On the other hand, bent chains could be warped chain galaxies. Along the lengths of the bent chains, the `pvector` intensity profiles are similar to those of other chain galaxies in the UDF, which are irregular with no exponential gradients (Elmegreen et al. 2004, 2005a).

The V_{606} surface brightnesses of the galaxies were also determined using the National Institutes of Health software package `imagej` (Rasband 1997), which allows measurement along a curved path. The average surface brightness in the interclump regions between the clumps is plotted for each galaxy versus $(1+z)^4$ in Figure 8. The intensity at a fixed rest-frame passband is expected to decrease from cosmological effects as the inverse of $(1+z)^4$, as shown by the dotted line (e.g., Lubin & Sandage

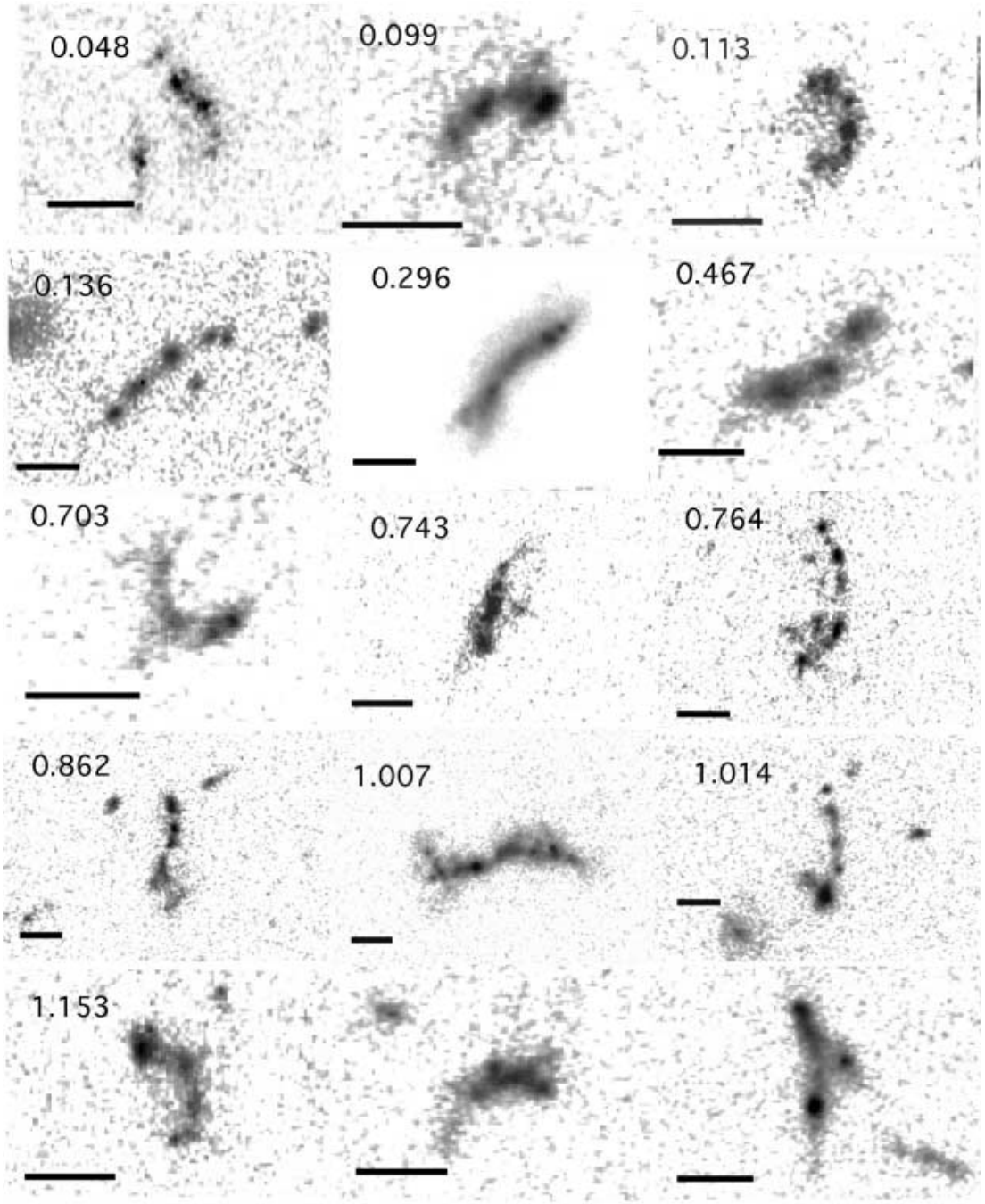

FIG. 3.—V_{606}-band images of bent chain galaxies in the GEMS and GOODS fields. Redshifts are in the upper left corner; horizontal lines represent 1″.

2001). With bandshifting in addition, the intensity could vary in a different way, depending on the star formation rate; higher rates produce intrinsically bluer galaxies and less of a decrease with $(1+z)^{-4}$.

Figure 8 suggests that the interclump intensities for the ring and partial ring galaxies are similar to each other and decrease slightly with increasing z, although not in proportion to $(1+z)^{-4}$. The spread in surface brightness for these galaxies is $\sim$1.5 mag arcsec^{-2} at each redshift. The bent chain galaxies are slightly different, having a nearly constant apparent interclump surface brightness, $\sim$24 mag arcsec^{-2}, independent of $(1+z)^4$ (except for one bent chain at $z = 0.296$, which is COMBO-17 No. 37539). This difference suggests that the interclump regions of bent chain galaxies have intrinsic surface brightnesses that increase rapidly with z, as a combined result of bandshifting into a relatively bright UV wavelength and increasing star formation rates with look-back time. The rings and partial rings have a more constant intrinsic interclump V_{606} surface brightness, which is dimmed by cosmological effects without as much offset from star formation.

3.2. *Clump Properties*

The clump sizes and separations were measured for each galaxy. The right panel of Figure 6 shows the clump diameter versus redshift for the GEMS and GOODS galaxies (the streaks correspond to integer numbers of pixels). The clump diameters do not depend noticeably on galaxy type. There is a correlation between minimum clump size and z, because of angular resolution limits. Figure 9 shows histograms of the ratio of the clump diameter to

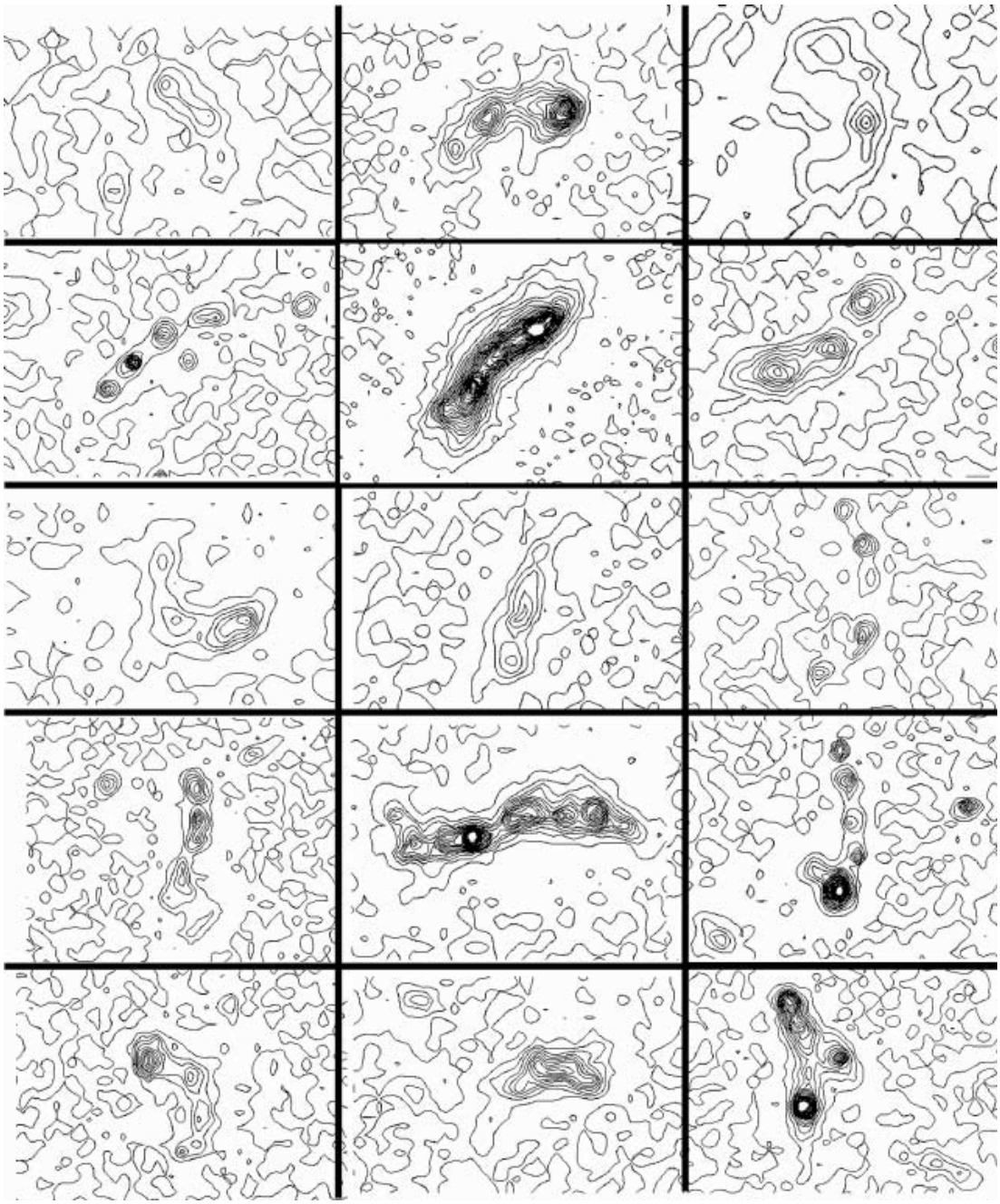

FIG. 4.—Plots of 2 σ contours of the bent chain galaxies in Fig. 3. The lowest contour (2 σ) is 25 mag arcsec^{-2}. There is no face-on component of a disk inside the arcs, suggesting that either the underlying disks are unusually faint, or these objects are unlike collisional or resonance ring galaxies.

the galaxy diameter. The histograms peak at ~0.08 galaxy diameters, regardless of galaxy type. The drop at lower relative size is probably from the resolution limit.

The clump separations are typically 1–3 clump diameters, and about 0.1–0.2 times the galaxy diameters. These sizes and proportions are consistent with the formation of clumps by gravitational instabilities in chain galaxies and collisional rings, considering that the ambient Jeans length is about the same as the clump separation. Collisional ring star formation has been modeled in detail by Struck-Marcell & Appleton (1987), Struck-Marcell & Higdon (1993), and others. Bent chains have the same clump sizes and relative separations as straight chains.

Figure 10 shows the apparent V_{606} clump magnitude as a function of redshift for the GEMS and GOODS ring, partial ring, chain, and bent chain galaxies (*left*), and for the UDF-chain and clump-cluster galaxies (*right*). The nuclei in the ring and partial ring galaxies (*diamonds in left panel*) have an apparent V_{606} magnitude of 24.5 ± 2 mag. Aside from the nuclei, the brightest GEMS and GOODS clumps in each morphology class are in the range from 25 to 26 mag, with no systematic trend in redshift. For the UDF clumps, the brightest are at ~26 mag, which is about the same. However, the faintest detected clumps are 2 mag brighter in GEMS and GOODS than they are in the UDF, as a result of the brighter detection limit of the GEMS and GOODS surveys. A more detailed examination of the GEMS and GOODS galaxies also revealed extremely faint clumps, but they are too faint to measure (e.g., COMBO-17 No. 47074 [$z = 0.837$] has very faint clumps in Fig. 1).

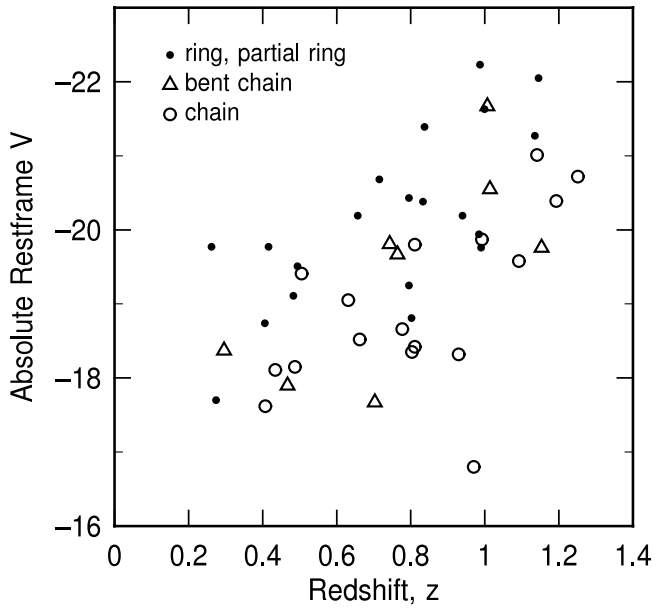

FIG. 5.—Absolute rest-frame *V*-band integrated magnitudes for ring and partial ring, bent chain, and chain galaxies in the GEMS and GOODS fields. The ring and partial ring galaxies are brighter on average than the chains and bent chains at a given redshift.

The rest-frame apparent (Fig. 10, *left*) and absolute (*right*) *B* magnitudes of the clumps are shown as a function of redshift in Figure 11 for galaxies in each sample. These rest-frame apparent magnitudes were found by interpolation between the observed passbands. For GEMS galaxies with z between 0.39 and 0.95, the rest-frame blue luminosity was taken to be $L_{B,\mathrm{rest}} = L_{V_{606}}(0.95 - z)/(0.95 - 0.39) + L_{z_{850}}(z - 0.39)/(0.95 - 0.39)$ for observed V_{606} and z_{850} luminosities. The rest-frame *B* magnitude is then $-2.5 \log L_{B,\mathrm{rest}}$. For GOODS and UDF galaxies, which have four observed passbands, the linear interpolation was done between each pair of passbands. We converted the apparent rest-frame magnitudes to absolute rest-frame magnitudes by applying the distance modulus determined from a ΛCDM cosmology (Spergel et al. 2003). For both the apparent and absolute magnitudes, the brightest clumps are equally bright in all galaxy types. The redshift trend for absolute magnitude is from the size cutoff; only the largest clumps can be seen at the highest redshift (Fig. 6), and these are the brightest.

Clump ages and masses were estimated from their V_{606}-z_{850} colors and magnitudes using Bruzual & Charlot (2003) spectral models that were redshifted and integrated over the filter functions of the ACS camera. We assumed models with a metallicity $Z = 0.008$ and a Chabrier (2003) IMF. Intervening hydrogen absorption was included following Madau (1995), and internal dust was included following Rowan-Robinson (2003), with extinction curves from Calzetti et al. (2000) and Leitherer et al. (2002). More details are given in Elmegreen & Elmegreen (2005).

Figure 12 shows the observed colors as a function of z for the ring and bent chain clumps in the GEMS and GOODS fields. The clump (V_{606}-z_{850}) colors generally range from 0 to 1 for all galaxies, with an average of 0.8 ± 0.6 for the ring clumps and 0.4 ± 0.4 for the bent chain clumps. There is a slight redshift dependence toward redder colors with increasing z for the ring and partial ring clumps. The superposed curves are models from Bruzual & Charlot, discussed above. The solid curves assume a clump age of 10^9 yr and four different star formation rate models: exponential decays with timescales of 10^7 (*top curve*), 3×10^8, and 10^9 yr, and a continuous star formation rate (*bottom curve*). The dashed curves assume a clump age of 10^8 yr, with four similar star formation rate models, as indicated, and the dotted curve assumes a clump age of 10^7 yr and an exponentially decaying star formation rate with a decay time of 10^7 yr.

The bent chain clumps are bluer than the ring and partial ring clumps for the same z, suggesting that the bent chain clumps are slightly younger than the ring clumps. Most of the bent chain clumps match models with ages of $\sim 10^7$ to $\sim 10^8$ yr for long decay times. Only one bent chain at $z \sim 0.7$ may have clumps as old as 10^9 yr. In contrast, clumps in the ring and partial ring galaxies are best matched by ages of 10^8 yr for various decay times, or 10^9 yr with a long decay time.

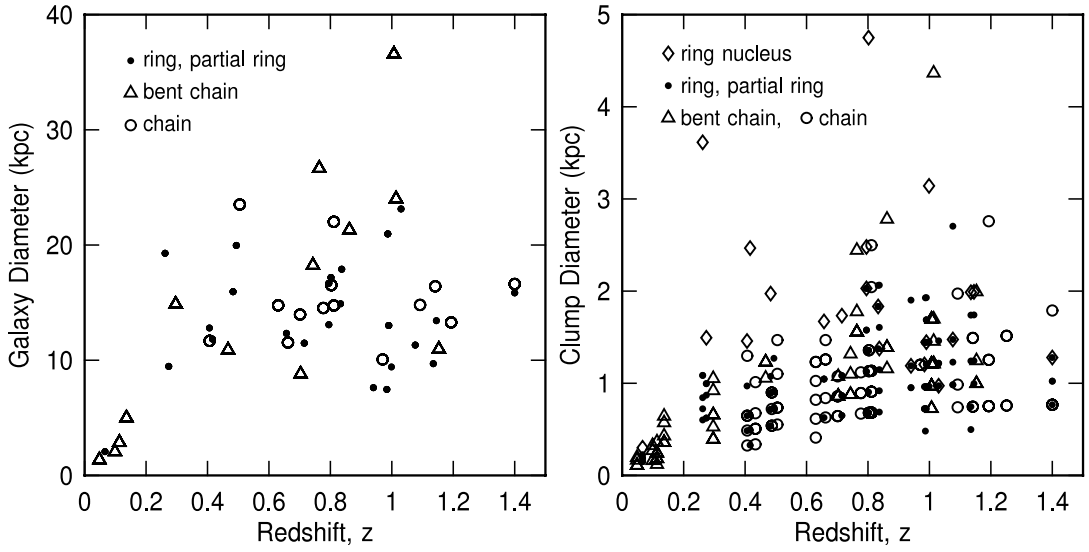

FIG. 6.—*Left:* Diameters of surveyed galaxies in the GEMS and GOODS fields. Above $z \sim 0.2$, there is no obvious correlation with redshift for any type. *Right:* Diameters of the clumps in the GEMS and GOODS galaxies vs. redshift. The band structure is from integer values of pixel size. The correlation is the result of decreasing spatial resolution with increasing z. There is no obvious difference in size for the various types. The ring galaxy nuclei (*diamonds*) are generally larger than the clumps.

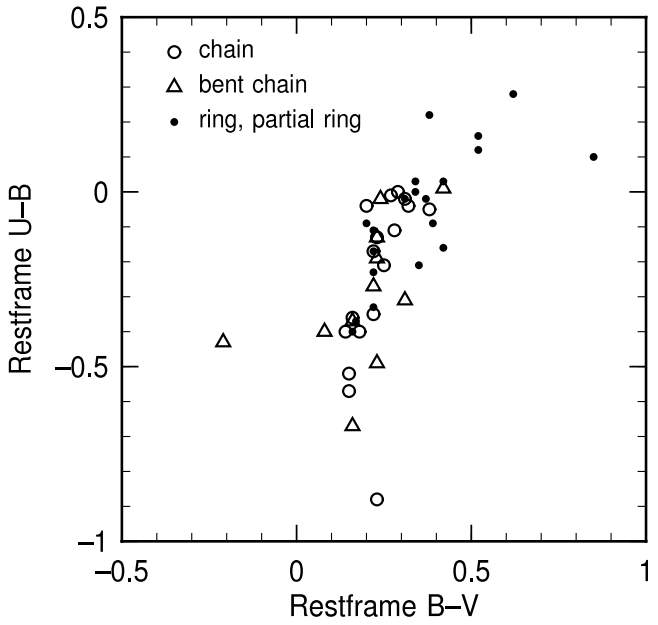

FIG. 7.—Rest-frame ($U-B$) and ($B-V$) integrated colors for ring and partial ring, bent chain, and chain galaxies in the GEMS and GOODS fields. The chain and bent chain galaxies are bluer than the ring and partial ring galaxies, suggesting younger average ages.

From the clump ages and apparent magnitudes, we can estimate masses from Bruzual & Charlot (2003) models, as shown in Figure 13. This figure plots mass versus clump age for a typical clump apparent magnitude of $V_{606} = 27$ (see Fig. 10), from which other magnitudes and masses can be scaled. Each curve is a different exponential decay time in a star formation model: 10^7 yr , 3×10^7 yr, 10^8 yr, 3×10^8 yr, 10^9 yr, and continuous (*top to bottom curves*). Considering the ages and decay times estimated in the previous paragraph and the apparent V_{606} magnitudes of the clumps, we infer that the clump masses average $\sim 5 \times 10^6\ M_\odot$ at low redshift to a few $\times\ 10^8\ M_\odot$ at $z \sim 1$. The clump masses are a factor of 2 or 3 lower for the bent chains than the ring and partial ring galaxies because, although the clump magnitudes are about the same, the bent chain clumps have slightly younger ages. Clump mass increases with redshift, as does the clump size and absolute magnitude discussed above, because of our size cutoff.

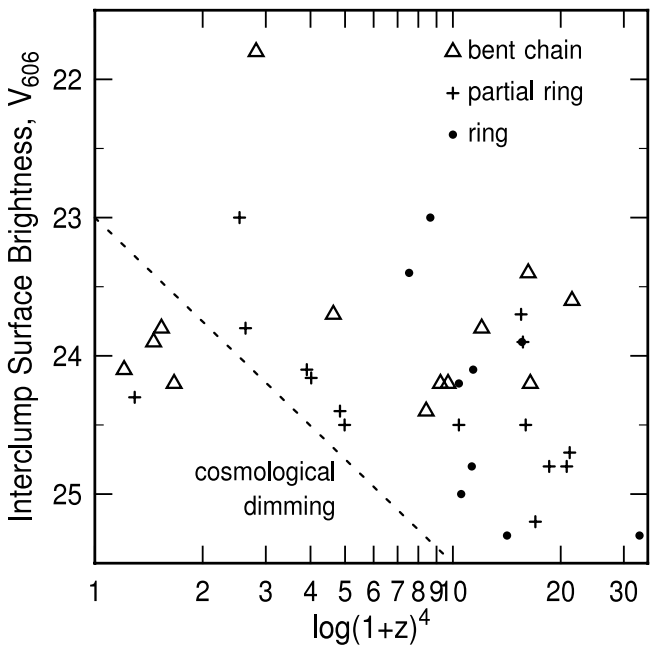

FIG. 8.—Apparent V_{606} surface brightnesses in mag arcsec^{-2} of the interclump regions as a function of $(1+z)^4$. The bent chains have a more constant V_{606} interclump surface brightness than the rings and partial rings, suggesting a difference in their average star formation properties.

3.3. *Comparison with Local Ring Galaxies*

3.3.1. *Collisional Ring Galaxies*

Several local collisional ring galaxies have ring morphologies similar to those in Figures 1 and 2. Some have off-center nuclei, and others are empty. Some resonance ring galaxies resemble our ring galaxies too. Because our GEMS and GOODS galaxies have redshifts averaging 0.78 ± 0.33, the rest frame is $\sim$3400 Å for the V_{606} images and 4800 Å for the z_{850} images. To make appropriate comparisons, we measured clumps in local galaxies from UV or B-band archival images.[2] Some of these images are at high resolution with *HST*, while others are from ground-based Schmidt or 5 m telescopes. The following nearby collisional ring galaxies were compared to our GEMS and GOODS sample: Arp 107, 146, 147, 148, 149; NGC 922; Cartwheel; AM 0644−74; and VII Zw 466 (+UGC 07683). For all of them, clump diameters ranged from 0.2 to 7 kpc (the latter with poor resolution), with a peak in the size distribution at 1.4 ± 1.8 kpc. The ratio of clump size to ring size was the same as for all the GEMS and GOODS samples, again peaking at about 0.1 (see Fig. 9).

The clumps in local collisional ring galaxies are bluer than the inner disks, as are the clumps in the GEMS and GOODS ring galaxies. For example, an optical study of several ring galaxies by Theys & Spiegel (1976) indicated ring colors similar to the blue colors of Magellanic-type irregulars. Analysis of the colors of 11 ring galaxies by Appleton & Marston (1997) showed that all of them have an outward blue gradient. Optical colors of clumps in VII Zw 466 suggested ages of $\sim 10^8$ yr, consistent with the inferred ring interaction age (Thompson & Theys 1978).

[2] See http://nedwww.ipac.caltech.edu/, as available.

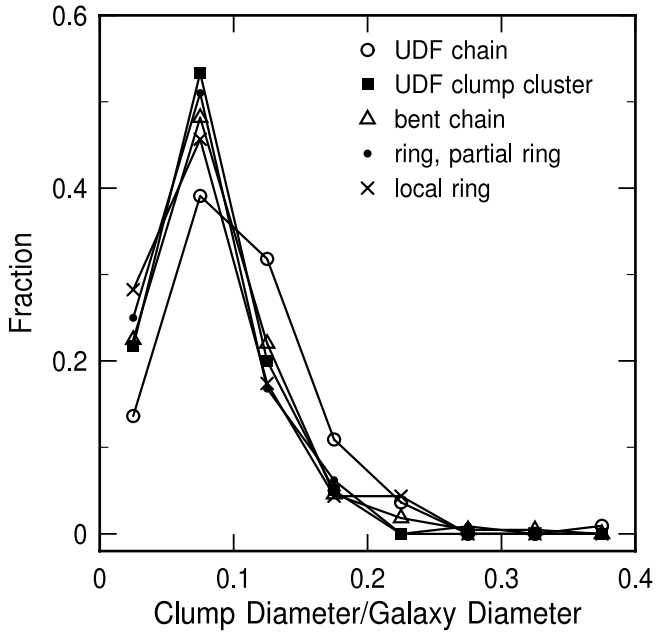

FIG. 9.—Clump sizes relative to the galaxy sizes for each type, including local ring galaxies. The relative sizes are comparable to or larger than 0.08.

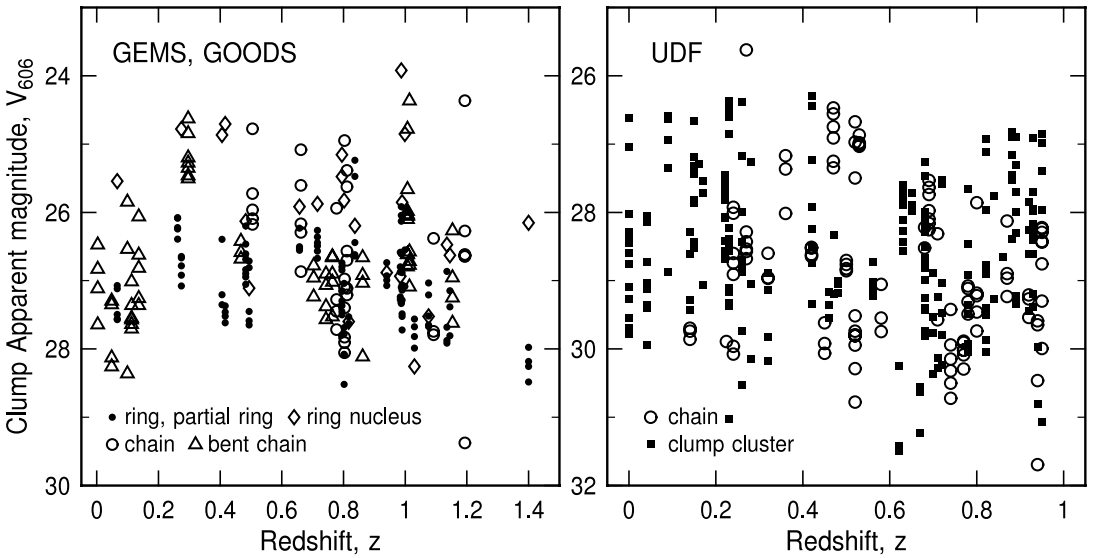

FIG. 10.—Observed V_{606} mag for nuclei and clumps in GEMS and GOODS ring, partial ring, chain, and bent chain galaxies (*left*) and for clumps in UDF clump-cluster and chain galaxies (*right*) as functions of redshift.

Three of the star-forming clumps in the ring of the Cartwheel galaxy (A0035 = Arp 10) have absolute B magnitudes of -17 to -18 mag, similar to the rest-frame absolute B clump magnitudes found here (Fig. 11); the total stellar mass associated with the H II regions is about $10^8\,M_\odot$ (Fosbury & Hawarden 1977). A similar object is the large southern ring galaxy AM 0644−741. It has massive star formation, apparently triggered in a double ring by a close encounter (Arp & Madore 1987). Higdon & Wallin (1997) used Hα measurements to infer star formation rates in AM 0644−741 and found a total new stellar mass of several $\times\,10^8\,M_\odot$ in the ring, considering the ring age of 110 Myr. These ages and masses are all similar to what we found for distant ring clumps.

Some local collisional ring galaxies show spokelike features that connect the inner cores to the rings, such as the Cartwheel and NGC 922. Although such features are difficult to discern in our distant galaxy sample, the top middle galaxy in Figure 2 (COMBO-17 No. 47074, $z = 0.837$) shows two inner arcs. Some of the others show hints of substructure also. Nonaxisymmetric features like these may grow from fragmentation and collapse of material in outwardly propagating waves (Hernquist & Weil 1993; Struck 1997). A barlike structure is seen in the top right galaxy in Figure 2 (No. 48709, $z = 0.494$). Huang & Stewart (1988) showed that a near-planar collision by an intruder can produce such a bar.

Several UDF clump cluster galaxies resemble local ring galaxies in having massive clumps in a circle around an empty center, as noted by Wong et al. (2006). Most clump clusters have irregularly placed clumps, however, so the fraction of these galaxies that might have collision or resonance rings is probably small.

The 25 galaxies identified as collisional ring galaxies in parallel fields out to $z = 1$ with WFPC2 F814W observations (Lavery et al. 2004) show many similarities to our GEMS and GOODS ring galaxies. Galaxies numbered 2, 8, 10, 11, 12, and 17 in their Figure 1 have symmetric rings and centered nuclei, like some of ours in Figure 1. The remainder of the Lavery et al. sample better match the partial ring galaxies in Figure 2.

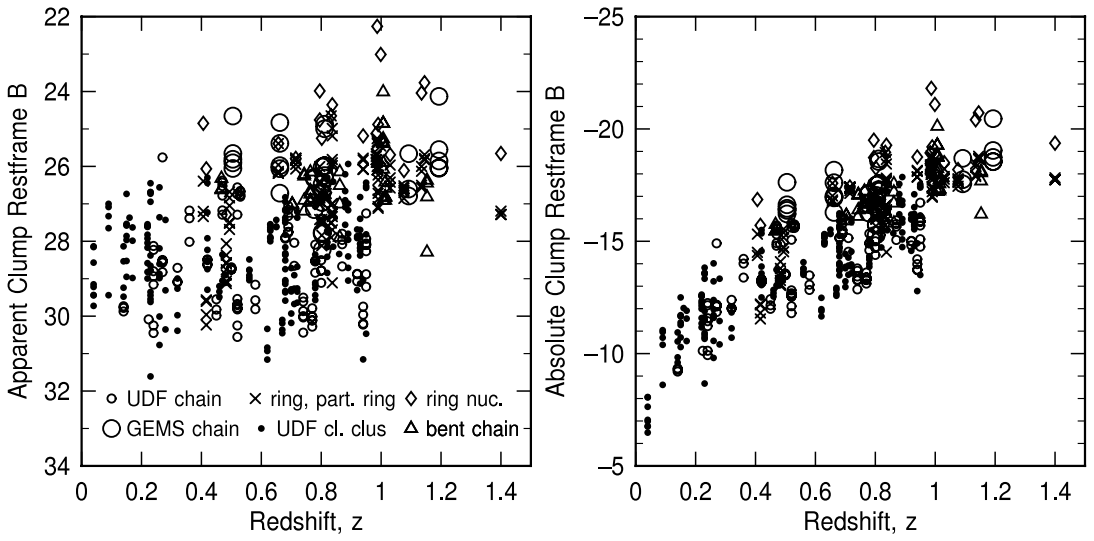

FIG. 11.—Rest-frame B-band apparent (*left*) and absolute (*right*) clump magnitudes vs. redshift for GEMS, GOODS, and UDF galaxies in the sample. The brightest clumps are equally bright in chain, clump-cluster, bent chain, and ring galaxies. Nuclei in ring and partial ring galaxies are indicated by diamonds.

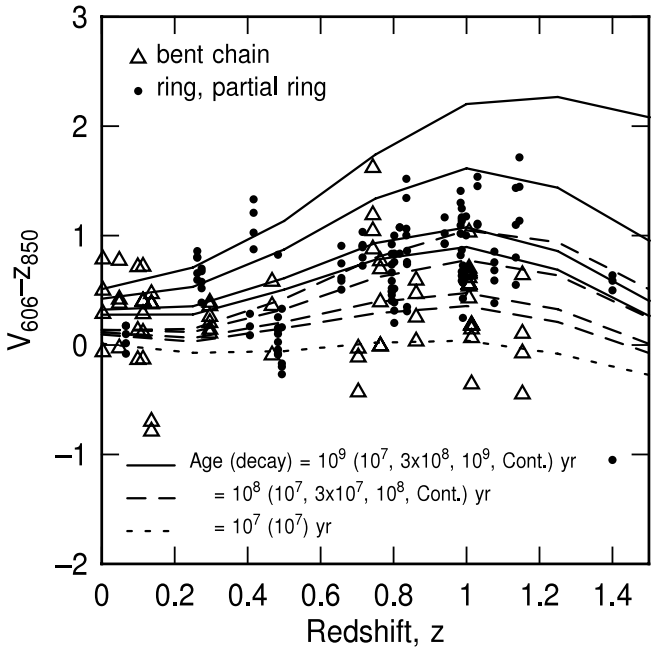

FIG. 12.—Observed ($V_{606}-z_{850}$) color vs. redshift z for ring and bent chain galaxy clumps in the GEMS and GOODS fields. Curves are models from Bruzual & Charlot (2003) with various clump ages and star formation decay times.

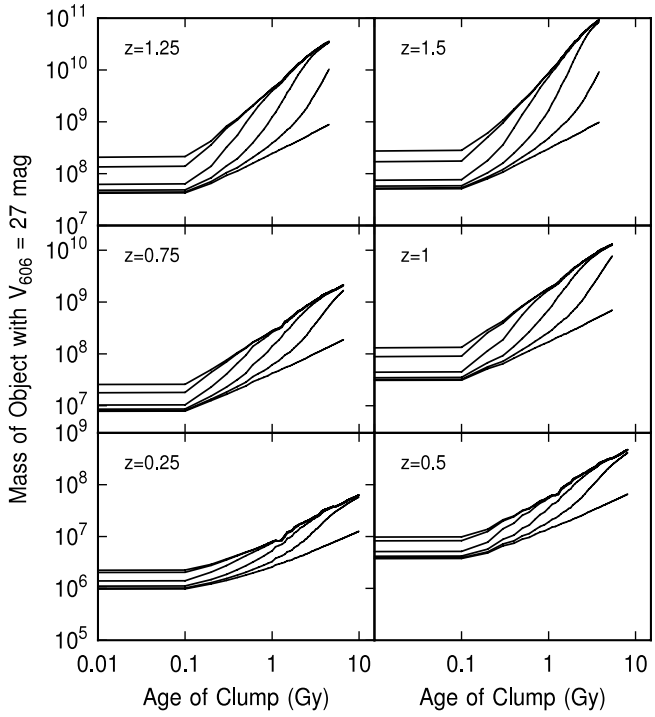

FIG. 13.—Expected mass as a function of star formation duration for a clump with an observed V_{606} mag of 27 for six different redshift bins. Star formation duration was estimated from a comparison of the previous two figures.

3.3.2. *Resonance Ring Galaxies*

Several of the galaxies in Figure 1 have symmetric rings with centered nuclei, making them look somewhat like local galaxies with strong outer resonance rings. For comparison, we examined the local outer ring galaxies IC 1993, NGC 6782, NGC 1433, IC 1438, and NGC 6753. The local rings are similar in size to the GEMS and GOODS rings, but the local star formation clumps in the rings are smaller and much fainter. The clumps in local resonance rings have average U- and B-band sizes equal to only $\sim$0.04 times the galaxy diameters, whereas the GEMS and GOODS clumps were typically comparable to or larger than 0.08 galaxy diameters (Fig. 9). Clump sizes that are as small as in local ring galaxies might not be resolved in the GEMS and GOODS fields, but still, the largest ring clumps at high redshift are larger than the largest ring clumps locally. This difference could be the result of a higher star formation rate in higher redshift galaxies. The local outer resonance ring galaxies tend to be early-type spirals, which have low star formation rates today.

Because bars can produce resonance rings, and bars are red, some of the GEMS and GOODS ring galaxies might have bars that cannot be seen at visible wave bands for our average $z \sim 0.78 \pm 0.33$. A mid-UV study of local galaxies (Windhorst et al. 2002) reveals that morphology is often similar from UV to optical, with a bar showing up in B as well as UV. Sometimes the change with passband is dramatic, however; in NGC 6782 the optical bar is visible out to B band, but disappears in the UV. While such a change is possible for our highest redshift galaxies, even at $z = 0.93$ we observe the rest-frame B band in the z_{850} images, and most bars should still be present there. Only seven of our ring and partial ring galaxies are at higher redshift than this. Thus, we looked for bars in our ring sample. A few of the galaxies in Figure 1 (*top left*: No. 53346, $z = 0.715$; *middle right*: No. 49092, $z = 0.802$; *bottom left*: No. 43780, $z = 0.833$; *bottom right*: No. 62696, $z = 1.40$) and Figure 2 (*top middle*: No. 34409, $z = 0.483$; *top right*: No. 48709, $z = 0.494$) show slight elongations in their centers that could be bars or oval distortions capable of producing an outer resonance ring. None of these bars is as prominent as the strong bars seen in today's SB0 ring galaxies (e.g., Buta & Combes 1996).

Collisional ring galaxies generally have small intruder galaxies nearby, so we examined the GEMS and GOODS fields surrounding the symmetric cases for possible companions. We found that four of the nine ring galaxies in Figure 1 (*top left*: No. 53346, $z = 0.715$; *middle*: No. 50905, $z = 0.795$; *bottom left*: No. 43780, $z = 0.833$; *bottom right*: No. 62696, $z = 1.40$) have small companions about 10 pixels in diameter, with redshifts differing from the ring galaxy by less than 0.1 and appearing within 1–3 galaxy diameters. These four cases could therefore have collisional rings and not resonance rings.

The galaxies without clear companions (Nos. 47074, 44999, 58535, 49092, 25076) are the most likely examples of resonance ring galaxies. Still, the morphology of these five candidates differs from the morphology of local outer-resonance ring galaxies. Only one of the five has an elongated nucleus that could be a bar (No. 49092, $z = 0.802$); the rest have small circular nuclei. This contrasts with local outer ring galaxies, which are mostly barred or have strong spiral arms. In de Vaucouleurs & Buta (1980), there are 46 galaxies with outer rings, and 17 with the A-type bar class (nominally, no bar). Of these, four looked barred after all, one is a strong merger with long tidal arms, four have flocculent arms throughout that are somewhat brighter in the ring region (but not a real ring), two others have spiral arms that wrap to an incomplete ring, and two have no visible ring.[3] The remaining three (NGC 1068, NGC 4736, NGC 3977) have smooth, weak outer rings and large, bright bulges and inner disks. These three local galaxies are the most similar to our four nonbarred outer ring candidates, although they are not identical. Also, the bar fraction for the best examples of local outer ring galaxies is very high, while it is only 20% in our sample. It is conceivable

[3] Based on B images in http://nedwww.ipac.caltech.edu/.

that our four nonbarred cases had bars when they formed their rings, and then the bars dissolved later. Such ring formation had to take ~6 Gyr or less for galaxies at $z \sim 0.8$. Why most of the local outer-resonance ring galaxies still have their bars when the distant ones do not is a mystery.

The average major-axis diameter of the five candidate resonance rings is 15 ± 5 kpc. The average diameter of the outer rings in 46 local galaxies in the ring catalog of de Vaucouleurs & Buta (1980) is 20 ± 10 kpc (using a Hubble constant of 71 km s^{-1} Mpc^{-1}). The local and high-redshift diameters are sufficiently close to each other that there could not have been a major change in outer ring position over the last ~6.6 Gyr, since $z = 0.78$. The slight increase seen here is consistent with an overall growth of galaxies over this time, by ~30% or so (with large uncertainties), or with a comparable slow down in the pattern speed for whatever drives the resonance.

Bar pattern speeds are expected to slow down as the bar transfers angular momentum to the halo (Debattista & Sellwood 1998; Athanassoula 2003). Athanassoula (2003) found that this interaction can slow down a bar in the last ~6 Gyr by 10%–40%, depending on the relative mass of the disk, bulge, and halo (see her Figs. 10 and 11). This range is consistent with the small increase in ring diameter found here for the same period of look-back time.

3.3.3. *Accretion Rings*

Other local analogs for the GEMS and GOODS galaxies are accretion rings (see Buta & Combes 1996), such as Hoag's Object, A1515+2146 (Schweizer et al. 1987), which either has a central E0 galaxy that accreted gas, or was once barred. Other accretion rings include the more commonly described Polar ring galaxies, which tend to have S0 galaxies in their centers and rings perpendicular to the disks (Whitmore et al. 1990). To match our observed galaxies, we would have to be viewing such a galaxy edge-on so the ring looks circular, but we do not see any extended central component that could be an edge-on spiral disk. Also, the atlas by Whitmore et al. shows that Polar rings tend to be much smoother than the clumpy rings of the GEMS and GOODS galaxies.

4. CONCLUSIONS

A total of 9 ring and 15 partial ring galaxies were found through visual examination of the GEMS and GOODS fields. An additional 15 bent chain galaxies were also observed. The clumps in the rings have diameters of ~1 kpc, depending on redshift. This is similar to the diameters of clumps in local collisional ring galaxies. The bent chains have rest-frame colors that are bluer than those in ring and partial ring galaxies. The individual clumps in the bent chain galaxies are also bluer than the clumps in rings and partial rings. The average star formation ages of the clumps in bent chains range from 10^7 to a few $\times 10^8$ yr; in the rings and partial rings, it is from a few $\times 10^8$ to 10^9 yr. Clump masses range from a few $\times 10^6$ to a few $\times 10^8$ $M_\odot$, with slightly lower values in bent chains. The measured clump mass increases with redshift because of resolution limits.

The morphologies and dimensions of local collisional ring galaxies are similar to the morphologies and dimensions of many of the ring galaxies in the GOODS and GEMS fields. Their clumps also have about the same sizes, ages, and masses. This similarity implies that many of the GEMS and GOODS rings and partial rings formed by plunging impacts of small companions through preexisting spiral galaxies.

Other galaxies in our sample, particularly the most isolated and symmetric and with the most centered nuclei, could have resonance rings instead of collisional rings. They differ from local resonance ring galaxies in having more star formation at high redshift, and therefore larger and bluer clumps in the rings. Some have slight indications of a bar, although the bar fraction seems lower for the best resonance ring cases than it is in the local universe. The existence of outer resonance rings in GOODS and GEMS galaxies implies that it takes only ~6 Gyr for the rings to form. After aging for another ~7 Gyr and avoiding disruptive collisions, they could turn into the modern versions of outer-resonance rings, which are smooth, red, and usually in early-type galaxies. If this is the case, then the similarity in diameter between the rings in our sample and the local outer resonance rings (local rings are ~30% larger) implies that spiral and bar pattern speeds have not changed by more than a factor of ~1.3 during last half of the life of the galaxy. This result may have important implications for nuclear gas accretion, which can speed up a bar, and bar-halo interactions, which can slow down a bar (Athanassoula et al. 2005). For example, bar-halo interactions studied by Athanassoula (2003) slow down a bar and extend the outer Lindblad resonance by about this much during the same time interval.

The bent chain galaxies in our survey differ from the ring galaxies, having younger, slightly less massive clumps and no evidence for an underlying, nearly face-on disk. The bent chains could be edge-on, clumpy, and bulge-free disks that got warped by an interaction. They resemble the straight chain galaxies that are observed in deep fields. Local disk galaxies do not have such large clumps as chains, nor are the local disks warped into similar arclike shapes.

D. M. E. thanks the staff at the Space Telescope Science Institute for their hospitality during her stay as a Caroline Herschel Visitor in October 2005. We thank the referee for useful suggestions about resonance ring galaxies.

REFERENCES

Abraham, R., Tanvir, N., Santiago, B., Ellis, R., Glazebrook, K., & van den Bergh, S. 1996a, MNRAS, 279, L47
Abraham, R., van den Bergh, S., Glazebrook, K., Ellis, R., Santiago, B., Surma, P., & Griffiths, R. 1996b, ApJS, 107, 1
Appleton, P., Charmandaris, V., & Struck, C. 1996, ApJ, 468, 532
Appleton, P., & Marston, A. 1997, AJ, 113, 201
Appleton, P., & Struck-Marcell, C. 1987, ApJ, 318, 103
Arp, H. J., & Madore, B. F. 1987, A Catalog of Southern Peculiar Galaxies and Associations (Cambridge: Cambridge Univ. Press)
Athanassoula, E. 2003, MNRAS, 341, 1179
Athanassoula, E., & Bosma, A. 1985, ARA&A, 23, 147
Athanassoula, E., Lambert, J. C., & Dehnen, W. 2005, MNRAS, 363, 496
Barnes, J., & Hernquist, L. 1992, ARA&A, 30, 705
Beckwith, S., et al. 2006, AJ, 132, 1729
Benitez, N. 2000, ApJ, 536, 571
Bruzual, G., & Charlot, S. 2003, MNRAS, 344, 1000
Buta, R., & Combes, F. 1996, Fundam. Cosm. Phys., 17, 95
Calzetti, D., Armus, L., Bohlin, R. C., Kinney, A. L., Koornneef, J., & Storchi-Bergmann, T. 2000, ApJ, 533, 682
Carroll, S. M., Press, W. H., & Turner, E. L. 1992, ARA&A, 30, 499
Chabrier, G. 2003, PASP, 115, 763
Coe, D., Benitez, N., Sanchez, S. F., Jee, M., Bouwens, R., & Ford, H. 2006, AJ, 132, 926
Conselice, C., Bershady, M., Dickinson, M., & Papovich, C. 2003, AJ, 126, 1183
Cowie, L., Hu, E., & Songaila, A. 1995, AJ, 110, 1576
Debattista, V. P., & Sellwood, J. A. 1998, ApJ, 493, L5
de Mello, D., Wadadeker, Y., Dahlen, T., Casertano, S., & Gardner, J. P. 2006, AJ, 131, 216
de Vaucouleurs, G., & Buta, R. 1980, AJ, 85, 637

Elmegreen, B. G., & Elmegreen, D. M. 2005, ApJ, 627, 632
Elmegreen, B. G., Elmegreen, D. M., Vollbach, D., Foster, E., & Ferguson, T. 2005a, ApJ, 634, 101
Elmegreen, D. M., Elmegreen, B. G., Ravindranath, S., & Coe, D. 2006, ApJ, submitted
Elmegreen, D. M., Elmegreen, B. G., Rubin, D. S., & Schaffer, M. A. 2005b, ApJ, 631, 85
Elmegreen, D. M., Elmegreen, B. G., & Sheets, C. 2004, ApJ, 603, 74
Few, J. M. A., & Madore, B. F. 1986, MNRAS, 222, 673
Fosbury, R. A. E., & Hawarden, T. G. 1977, MNRAS, 178, 473
Fukugita, M., Shimasaku, K., & Ichikawa, T. 1995, PASP, 107, 945
Giavalisco, M., et al. 2004, ApJ, 600, L103
Hernquist, L., & Weil, M. 1993, MNRAS, 261, 804
Higdon, J., & Wallin, J. 1997, ApJ, 474, 686
Huang, S.-N., & Stewart, P. 1988, A&A, 197, 14
Korchagin, V., Mayya, Y. D., & Vorobyov, E. 2001, ApJ, 554, 281
Lavery, R., Remijan, A., Charmandaris, V., Hayes, R., & Ring, A. 2004, ApJ, 612, 679
Leitherer, C., Li, I.-H., Calzetti, D., & Heckman, T. M. 2002, ApJS, 140, 303
Lotz, J. M., et al. 2006, ApJ, in press (astro-ph/0602088)
Lubin, L. M., & Sandage, A. 2001, AJ, 122, 1084
Lynds, R., & Toomre, A. 1976, ApJ, 209, 382
Madau, P. 1995, ApJ, 441, 18
Mihos, C., & Hernquist, L. 1994, ApJ, 437, 611
Neuschaefer, L., Im, M., Ratnatunga, U., Griffiths, R., & Casertano, S. 1997, ApJ, 480, 59
Rasband, W. S. 1997, ImageJ (Bethesda: NIH), http://rsb.info.nih.gov/ij/
Rix, H. W., et al. 2004, ApJS, 152, 163
Rowan-Robinson, M. 2003, MNRAS, 345, 819
Schweizer, F., Ford, W. K., Jedrzejewski, R., & Giovanelli, R. 1987, ApJ, 320, 454
Smith, B. J., Struck, C., Appleton, P. N., Charmandaris, V., Reach, W., & Eittier, J. J. 2005, AJ, 130, 2117
Spergel, D. N., et al. 2003, ApJS, 148, 175
Straughn, A., Cohen, S., Ryan, R., Hathi, N., Windhorst, R., & Jansen. R. 2006, ApJ, 639, 724
Struck, C. 1997, ApJS, 113, 269
———. 1999, Phys. Rep., 321, 1
Struck, C., Appleton, P., Borne, K., & Lucas, R. 1996, AJ, 112, 1868
Struck-Marcell, C., & Appleton, P. 1987, ApJ, 323, 480
Struck-Marcell, C., & Higdon, J. L. 1993, ApJ, 411, 108
Theys, J. C., & Spiegel, E. A. 1976, ApJ, 208, 650
———. 1977, ApJ, 212, 616
Thompson, L., & Theys, J. 1978, ApJ, 224, 796
Whitmore, B. C., Lucas, R. A., McElroy, D. B., Steiman-Cameron, T. Y., Sackett, P. D., & Olling, R. P. 1990, AJ, 100, 1489
Windhorst, R. A., et al. 2002, ApJS, 143, 113
Wolf, C., Meisenheimer, K., Rix, H.-W., Borch, A., Dye, S., & Kleinheinrich, M. 2003, A&A, 401, 73
Wong, O., et al. 2006, MNRAS, 370, 1607